Naval Research Laboratory
Washington, DC 20375-5000

NRL Memorandum Report 6140

SARLAC: A Relativistic Electron Beam Code

GLENN JOYCE, RICHARD HUBBARD,
MARTIN LAMPE, AND STEVEN SLINKER

Plasma Physics Division

February 10, 1988

SECURITY CLASSIFICATION OF THIS PAGE

REPORT DOCUMENTATION PAGE

Form Approved
OMB No 0704-0188

1a REPORT SECURITY CLASSIFICATION: UNCLASSIFIED	1b RESTRICTIVE MARKINGS:
2a SECURITY CLASSIFICATION AUTHORITY:	3 DISTRIBUTION/AVAILABILITY OF REPORT: Approved for public release; distribution unlimited.
2b DECLASSIFICATION/DOWNGRADING SCHEDULE:	
4 PERFORMING ORGANIZATION REPORT NUMBER(S): NRL Memorandum Report 6140	5 MONITORING ORGANIZATION REPORT NUMBER(S):
6a NAME OF PERFORMING ORGANIZATION: Naval Research Laboratory; 6b OFFICE SYMBOL (If applicable): 4790	7a NAME OF MONITORING ORGANIZATION: Naval Surface Weapons Center
6c ADDRESS (City, State, and ZIP Code): Washington, D.C. 20375-5000	7b ADDRESS (City, State, and ZIP Code): Silver Spring, MD 20903-5000
8a NAME OF FUNDING/SPONSORING ORGANIZATION: DARPA; 8b OFFICE SYMBOL (If applicable):	9 PROCUREMENT INSTRUMENT IDENTIFICATION NUMBER: 47-0900-0-7
8c ADDRESS (City, State, and ZIP Code): Arlington, VA 22209	10 SOURCE OF FUNDING NUMBERS: PROGRAM ELEMENT NO 62707E; PROJECT NO N60921-86-WR-W0233; TASK NO ARPA Order #4395,A63; WORK UNIT ACCESSION NO DN680-415

11 TITLE (Include Security Classification)
SARLAC: A Relativistic Electron Beam Code

12 PERSONAL AUTHOR(S)
Joyce, Glenn, Hubbard, Richard, Lampe, Martin, and Slinker, Steven

13a TYPE OF REPORT	13b TIME COVERED	14 DATE OF REPORT (Year, Month, Day)	15 PAGE COUNT
Interim	FROM _____ TO _____	1988 February 10	26

16 SUPPLEMENTARY NOTATION

17 COSATI CODES		
FIELD	GROUP	SUB-GROUP

18 SUBJECT TERMS (Continue on reverse if necessary and identify by block number)
relativistic electron beams; hose instability; particle simulation code; beam propagation code.

19 ABSTRACT (Continue on reverse if necessary and identify by block number)

SARLAC is a particle simulation code for studying the propagation of ultra-relativistic electron bears. It is used to study the nonlinear evolution of the resistive hose instability. We have developed a fast, semi-implicit, iterative field solver which allows us to include a large number of Fourier modes in the azimuthal direction. The solver iterates about a solution of the field equations dominated by the axisymmetric (m = 0) conductivity. This technique has proved to be quite successful. We compare some results of the code with those obtained from a linear-ized hose simulation code, and show differences when the hose oscillations reach large amplitude. Keywords:

20 DISTRIBUTION/AVAILABILITY OF ABSTRACT	21 ABSTRACT SECURITY CLASSIFICATION
☒ UNCLASSIFIED/UNLIMITED ☐ SAME AS RPT ☐ DTIC USERS	UNCLASSIFIED
22a NAME OF RESPONSIBLE INDIVIDUAL: Glenn Joyce	22b TELEPHONE (Include Area Code): (202) 767-6785; 22c OFFICE SYMBOL: 4790

DD Form 1473, JUN 86 — Previous editions are obsolete — S/N 0102-LF-014-6603

CONTENTS

ELECTROMAGNETIC FIELDS 2

NUMERICAL ISSUES 6

NUMERICAL RESULTS 9

ACKNOWLEDGMENTS 10

REFERENCES 11

SARLAC: A RELATIVISTIC ELECTRON BEAM CODE

We have recently written a number of simulation codes to test various aspects of the resistive hose instability in high energy electron beams propagating in resistive plasmas. Most methods used previously for treating the instability were restricted to small instability amplitudes. These are considered to be of practical interest because large amplitude hose-like oscillations quickly destroy the integrity of the the beam, and because, under appropriate circumstances, the instability "saturates" in the linear regime. That is to say, the hose instability is convective in the beam frame, and therefore, at any given point in the beam may reach a maximum which is still small followed by a decay of the instability as the disturbance convects past. Near term experiments, however, are frequently more unstable than can be treated by linear models, so we have developed a particle simulation code which can follow the evolution of an instability into the nonlinear regime[1-3]. Similar codes have been written by Godfrey[4] and Freeman[5].

The nonlinear code has borrowed heavily from two of our previous codes, SIMM0[6] and SIMM1[7] which are particle simulation codes for axi-symmetric beams and beams with small amplitude hose motions. The particle dynamics of those two codes are followed in Cartesian coordinates so the SARLAC code differs from these primarily in the calculation of the electromagnetic fields. We have developed a fast iterative field solver which allows us to include a large number of Fourier modes in the azimuthal direction.

The code employs many of the approximations found in most linearized propagation models[8-10]. The variables z and t are replaced by z and $\zeta = ct - z$ (the distance from the beam head), and all particles remain at constant ζ since v_z is assumed to be the velocity of light. The frozen approximation is used in the field equations, and the same conductivity

Manuscript approved October 7, 1987.

model used in the VIPER[8] code is employed. Beam dynamics are treated using standard particle simulation techniques. Current densities, fields, and conductivity are calculated on a polar grid (u,Θ,ζ) with $u = \sqrt{r}$ as the radial variable. The lay-down scheme for the particles is quadratic in the radial and azimuthal variables and nearest grid point in the axial variable.

The ultra-relativistic approximations used in SARLAC lead to a code structure which is substantially different from "conventional" particle simulations. Information can only flow in one direction; toward larger ζ. Also, since individual particles always remain at the same axial position within the beam, the simulation can treat one slice at a time, thus reducing the number of particles in the simulation at any one time to $\sim 10^4$. Each beam slice is propagated forward in z until the maximum propagation range, z_{max} is reached. At this point, particles are loaded into the next slice, and the process is repeated. The current density J, conductivity σ, and potentials A and ϕ from the previous slice must be read from disk. The axial step $\Delta\zeta$ is variable, and the code has the option of subgridding the field and conductivity integrations on a finer axial mesh than is used for the particles. All diagnostics are done with post-processors. The dimensionless units used in VIPER and SIMM1 are employed throughout[7,8].

ELECTROMAGNETIC FIELDS

The frozen approximation to Maxwell's equations is performed in a gauge suggested by Lee[11]. The equations are

$$\nabla_\perp^2(a + \phi) - \frac{\partial^2 a}{\partial \zeta^2} = - J_b + \sigma \frac{\partial a}{\partial \zeta}, \tag{1}$$

$$- \nabla_\perp^2 \frac{\partial a}{\partial \zeta} = - \nabla_\perp \cdot (\sigma \nabla_\perp \phi), \tag{2}$$

with the frozen condition

$$\frac{\partial}{\partial \zeta} \vec{A}_\perp = \frac{\partial a}{\partial z} = \frac{\partial \phi}{\partial z} = \frac{\partial \vec{A}_\perp}{\partial z} = 0 \tag{3}$$

and $a = A_z - \phi$.

The boundary conditions for a and ϕ are

$$a(r) = 0 , \quad \zeta = 0$$

$$\phi(r) = 0 , \quad \zeta = 0$$

$$a(\zeta) = 0 , \quad r = R_{max}$$

$$\phi(\zeta) = 0 , \quad r = R_{max}.$$

These conditions correspond to a beam propagating at the speed of light in a perfect conductor of radius R_{max}.

The equations are similar in form to the EMPULSE[12] equations with an additional term $\partial^2 a/\partial \zeta^2$ in the first equation. A fully implicit method for solving these equations has been developed by Hui[13]. That field solver Fourier analyzes the azimuthal dependence of all quantities into a series of modes $\exp(im\Theta)$ and performs a full complex matrix inversion, which is extremely time consuming and thus impractical for long simulation studies. The major advance of the SARLAC code is the development of a field solver which does not require a complete matrix inversion. The SARLAC field solver uses a predictor-corrector method which iterates about a solution obtained by assuming that the axi-symmetric (m = 0) conductivity dominates the solution. The m = 0 mode of any positive definite function is always larger than any other single mode and in the case of beam generated conductivity which is generated all along the beam axis, this mode is large compared to the other modes even for large excursions of the beam from axi-symmetry, as long as the front of the beam is on the axis.

Consider the first equation, and write it in the form

$$e^{-\int \sigma d\zeta'} \frac{\partial}{\partial \zeta} e^{\int \sigma d\zeta'} \frac{\partial a}{\partial \zeta} = \nabla_\perp^2 (a + \phi) + J_b. \tag{4}$$

Integrate this equation over the interval $\zeta_n \le \zeta \le \zeta_{n+1}$ to obtain

$$a^{n+1} = \left\{a^n - a^{n-1}\,\frac{1}{2\sigma\Delta\zeta}\left(1 - e^{-\sigma\Delta\zeta}\right) + J_b\,\frac{1}{\sigma^2}\left(\sigma\Delta\zeta - \left(1 - e^{-\sigma\Delta\zeta}\right)\right)\right.$$

$$\left. + \nabla_\perp^2(a + \phi)\,\frac{1}{\sigma^2}\left(\sigma\Delta\zeta - \left(1 - e^{-\sigma\Delta\zeta}\right)\right)\right\} \Big/ \left(1 - \frac{1}{2\sigma\Delta\zeta}\left(1 - e^{-\sigma\Delta\zeta}\right)\right), \quad (5)$$

where the superscript n represents the function evaluated at ζ_n. The conductivity, σ, is evaluated in the interval (ζ_n, ζ_{n+1}). Rewrite Eq. (5) as

$$a^{n+1} = F(a^n, a^{n-1}; J_b, \sigma)$$

$$+ \nabla_\perp^2(a + \phi) f(\sigma), \quad (6)$$

where

$$F(a^n, a^{n-1}; J_b, \sigma) = \left\{a^n - a^{n-1}\,\frac{1}{2\sigma\Delta\zeta}\left(1 - e^{-\sigma\Delta\zeta}\right)\right.$$

$$\left. + J_b\,\frac{1}{\sigma^2}\left(\sigma\Delta\zeta - \left(1 - e^{-\sigma\Delta\zeta}\right)\right)\right\} \Big/ \left(1 - \frac{1}{2\sigma\Delta\zeta}\left(1 - e^{-\sigma\Delta\zeta}\right)\right) \quad (7)$$

and

$$f(\sigma) = \frac{\left(\sigma\Delta\zeta - \left(1 - e^{-\sigma\Delta\zeta}\right)\right)/\sigma^2}{\left(1 - \frac{1}{2\sigma\Delta\zeta}\left(1 - e^{-\sigma\Delta\zeta}\right)\right)}. \quad (8)$$

Note that

$$f(\sigma) \longrightarrow \Delta\zeta/\sigma \qquad \text{for } \sigma \text{ large}$$

$$f(\sigma) \longrightarrow (\Delta\zeta)^2 \qquad \text{for } \sigma \text{ small.}$$

Equation (2) is simply differenced to give

$$-\nabla_\perp^2\,\frac{a^{n+1} - a^n}{\Delta\zeta} = -\nabla_\perp\cdot(\sigma\nabla_\perp\phi). \quad (9)$$

Note that we have omitted the superscripts from some of the a and ϕ terms in Eqs. (6) and (9). By choosing these terms at the nth or (n+1)th (or some combination of these levels), the differencing can be made explicit, or implicit to some formal accuracy. Our experience has been that the algorithms for these equations are numerically unstable if they are explicitly differenced. An implicit differencing can eliminate the instability, but at the expense of a complicated matrix inversion due to the azimuthal coupling of σ with the potentials. To avoid this, we have chosen instead to to rewrite Eqs. (6) and (9) as

$$a^{n+1} - \nabla_\perp^2(a + \phi)\, f_0(\phi) = F(a^n, a^{n-1}; J_b, \phi)$$

$$+ \nabla_\perp^2(a + \phi)\left[f(\phi) - f_0(\phi)\right] \qquad (10)$$

and

$$- \nabla_\perp^2 \frac{a^{n+1} - a^n}{\Delta\zeta} + \nabla_\perp\cdot(\sigma_o \nabla\phi) = - \nabla_\perp\cdot(\sigma - \sigma_o)\nabla_\perp\phi, \qquad (11)$$

where

$$f_0(\sigma) = \frac{1}{2\pi}\int_0^{2\pi} f\,(\sigma(\theta) d\,\theta,\ \sigma_0 = \frac{1}{2\pi}\int_0^{2\pi} \sigma\,(\theta)\, d\theta \qquad (12)$$

Equations (10) and (11) are formally the same as Eqs. (6) and (9). However, since σ_o does not vary in azimuth, the left-hand sides of these equations can be evaluated at the upper level without involving convolution sums, which leads to a tri-diagonal form for a^{n+1} and ϕ^{n+1}. The right-hand sides can be evaluated explicitly since the functions are known. The simplest differencing scheme leads to a first order algorithm. We have chosen a predictor-corrector method which is accurate to second order and quite stable. For the sake of brevity, we will not go into the details of

the differencing, but they are easily reproduced. We solve the equations in the Fourier transformed space (u,m,ζ) always keeping the right-hand sides explicit. The right-hand sides, then, can be evaluated in (u,Θ,ζ) thus avoiding convolution sums on the right-hand sides as well. The method of adding and subtracting averaged terms to gain stability without full matrix inversions is similar to that used by Harned[14] for a different set of equations.

NUMERICAL ISSUES

In SARLAC, the number of modes N_Θ and radial mesh size Δu remain fixed throughout a run. Typically, $N_\Theta = 16$ or 32, and $\Delta u = 0.125\ a_o^{1/2}$, where a_o is a characteristic initial beam radius. The axial grid spacing $\Delta\zeta$ is specified for each slice at the beginning of the run. In general, $\Delta\zeta$ is allowed to increase with ζ since (at least in the linear regime) the ζ-variation is characterized by the dipole decay length, $\pi\sigma(r=0)a_o^2/2c^2$, which usually increases monotonically throughout the pulse. However, field solver tests have shown that the axial step size must often be reduced when the beam displacement is large. This is accomplished by subgridding the field and conductivity integrations. In most cases, $\Delta\zeta$ is chosen to be small enough that subgridding is rarely involved.

The beam current density J_b is intrinsically noisy because of the statistical fluctuations arising from the small number of particles in each u-Θ grid cell. This is particularly troublesome near $u = 0$. Increasing the number of simulation particles per slice reduces noise problems but is computationally expensive. Other methods which we have employed include accumulating current densities on a coarser radial mesh than is used for the field solver and interpolating, averaging over the first few radial grid points, and using an azimuthal filtering technique near the origin.

Originally, we assigned random initial values of Θ to the particles but found that this procedure resulted in large initial noise levels for the hose instability and in substantial drifts in the beam head. The noise effects are reduced by loading the particles in pairs on opposite sides of the beam. If the velocities are also loaded symmetrically, the m = 1 azimuthal mode is eliminated in the initial stages of propagation. A small specified perturbation can be added to all particles in a given beam slice to start the hose instability in a controlled manner. Higher order Fourier modes can be suppressed by loading four or more particles with the appropriate symmetry. The elimination of higher order modes has not proven particularly useful since the nonlinear coupling of these modes is usually too weak to introduce significant hose growth.

The scattering of beam electrons by the neutral gas is known to play an important role in the evolution of the beam. SARLAC uses an algorithm originally developed by Chambers[6,15] and modified by Hughes and Godfrey[16] to provide a more accurate representation of the scattering process. Each beam particle is periodically scattered through a randomly chosen angle whose characteristic magnitude is determined by the energy and the gas density. After an initial transient phase, the beam reaches a quasi-static equilibrium. The beam radius then expands slowly due to scattering. If beam particles are loaded in pairs, a straightforward application of the scattering algorithm will eventually introduce significant noise and drifts at the beam head. These effects can be eliminated by scattering the particles in pairs. The random velocity $\Delta\vec{v}_i$ applied to a given particle at a given z step is balanced by adding $-\Delta\vec{v}_i$ to the particle with which it was originally paired. This technique has been highly successful in practice.

The simulation code is best suited for treating cases in which the hose displacement is a few times the nominal radius a_o. The coordinate system is chosen to have the finest resolution in both the radial and azimuthal directions near the origin. For extremely large beam oscillations, when the beam displacement reaches a substantial fraction of the wall radius, the accuracy of the simulation is reduced, and the field solver is sometimes subject to numerical instabilities. The field solver instabilities appear to be triggered by conditions in which the local conductivity centroid gets far enough off the coordinate system axis that the conductivity is not dominated by the m = 0 mode. Usually this conductivity is generated by avalanche due to strong, localized, electric fields; such fields can arise when the hose motion is quite nonlinear[1]. Evidence for very strong electric fields associated with nonlinear hose motion has been seen in the ETA experiments[17], so the strong fields may be physical (up to a point). Considerable effort has been made to make the field solver more robust, and with careful differencing we have had some success. We have also found that these problems can be mitigated by using small ζ grids in regions where there are large hose amplitudes. Even so, we believe the code to be best suited for moderate hose oscillations.

NUMERICAL RESULTS

We have run the code under a variety of conditions. We show here the results of two runs; one for small perturbations in which the hose stays in the linear regime, saturates and decays, and one with moderate initial perturbations for which the hose grows and becomes nonlinear. The parameters for both sets of runs are

a_o = .5 cm, the beam radius.

I = 10 kA, the beam current.

γ = 100, the beam energy.

ζ_r = 15 cm, the beam current rise length.

a_w = 81 a_o, the outer radius of the simulation.

$y_{pert} = y_o \sin 2\pi ((\zeta-\zeta_o)/\zeta_o)$, the initial perturbation over the range

$$\zeta_o < \zeta < 1.5\ \zeta_o,\ \zeta_o = 10 \text{ cm}.$$

(Note, this perturbation is in the y direction.)

For the first run we used a very small initial hose amplitude $y_o = 10^{-5} a_o$ which kept the hose oscillations linear over the length of the beam. For this case, the hose instability grows and saturates as seen in Fig. 1. Figure 2 shows a comparison of the saturation amplitude at various distances from the beam head with the results of the linearized VIPER code, which uses the multi-component model[18] to represent the particle dynamics approximately. The oscillation frequency, growth rate, and saturation amplitude agree quite well with the VIPER code[8].

The parameters chosen for the second run were the same except for a much larger initial amplitude $y_o = 10^{-2} a_o$, so that the hose oscillations would become nonlinear. Figure 3 shows the growth of the hose through the x and y centroids of the beam. The dashed line is the y centroid which is

much larger than x because the perturbation is initialized in y. After the hose displacements reach the order of the beam radius, the frequency of the oscillation decreases. This is because the beam is spreading in radius and the wavelength of the oscillation scales as the radius. Figures 4-6 are beam particle plots at various distances of propagation.* We can see the development of the hose instability and the loss of the beam pinch as the instability becomes large.

Acknowledgments

We would like to thank Drs. Bertram Hui and Richard Fernsler for their work on the code models and to Dr. Wahab Ali for his contributions to the conductivity model. We also want to acknowledge Dr. Keith Brueckner, Frank Chambers, William Fawley, Leon Feinstein, John Freeman, Brendan Godfrey, William Sharp, and John Wagner, all of whom had an influence on the development of the code.

This work was supported by the Defense Advanced Research Projects Agency under ARPA Order No. 4395, Amendment No. 63, and monitored by the Naval Surface Weapons Center.

*To optimize the visual density of the plots, a randomly selected subset of the beam particles are plotted, rather than the entire beam.

REFERENCES

1. R. F. Fernsler, R. F. Hubbard, B. Hui, G. Joyce, M. Lampe, and Y. Y. Lau, Phys. Fluids 29, 3056 (1986).
2. R. F. Hubbard, G. Joyce, S. P. Slinker, M. Lampe, and J. M. Picone, Bull. Am. Phys. Soc. 30, 1583, (1985).
3. R. F. Hubbard, S. P. Slinker, G. Joyce, and M. Lampe, Bull. Am. Phys. Soc. 31, 1429 (1986).
4. B. B. Godfrey, M. M. Campbell, B. S. Newberger, L. A. Wright, and C. A. Ekdahl, Mission Research Corp., AMRC-R-671 (1985).
5. J. R. Freeman, J. W. Poukey, J. S. Wagner, and R. S. Coats, J. Appl. Phys. 59, 725, (1986).
6. G. Joyce and M. Lampe, Phys. Fluids 26, 3377 (1983).
7. G. Joyce and M. Lampe, J. Comp. Phys., 63, 398, (1986).
8. M. Lampe, W. M. Sharp, R. F. Hubbard, E. P. Lee and R. H. Briggs, Phys. Fluids 27, 2921 (1984).
9. E. P. Lee, F. W. Chambers, L. L. Lodestro and S. S. Yu, Proc. of the 2nd Intl. Topical Conf. on High Power Electron Beam Research and Technology (Cornell Univ., Ithaca, NY) Vol. I, p. 381 (1977).
10. R. L. Feinstein, D. A. Keeley, E. R. Parkinson and W. Reinstra, Science Applications International Corp. Report SAIC-U-74-PA-DOE (1984).
11. W. S. Sharp, S. S. Yu, and E. P. Lee, Lawrence Livermore National Laboratory, Report UCID-21114, (1987).
12. E. P. Lee, Lawrence Livermore National Laboratory, Report UCID-17286 (1976).
13. B. Hui and M. Lampe, J. Comp. Phys., 55 (1984).
14. D. S. Harned and W. Kerner, J. Comp. Phys. 60 1 62 (1985).

15. F. W. Chambers Lawrence Livermore National Laboratory Report UCID-18302, (1979).

16. T. P. Hughes and B. B. Godfrey, Phys. Fluids. 27, 1531, (1984).

17. J. C. Clark, K. W. Struve, S. S. Yu, and R. E. Melendez, Proc. of the 5th Intl. Conf. on High-Power Particle Beams, edited by R. J. Briggs and A. J. Toepfer (Lawrence Livermore National Laboratory, Livermore, 1983), p. 412.

18. W. M. Sharp, M. Lampe, H. S. Uhm, Phys. Fluids. 25, 1456 (1984).

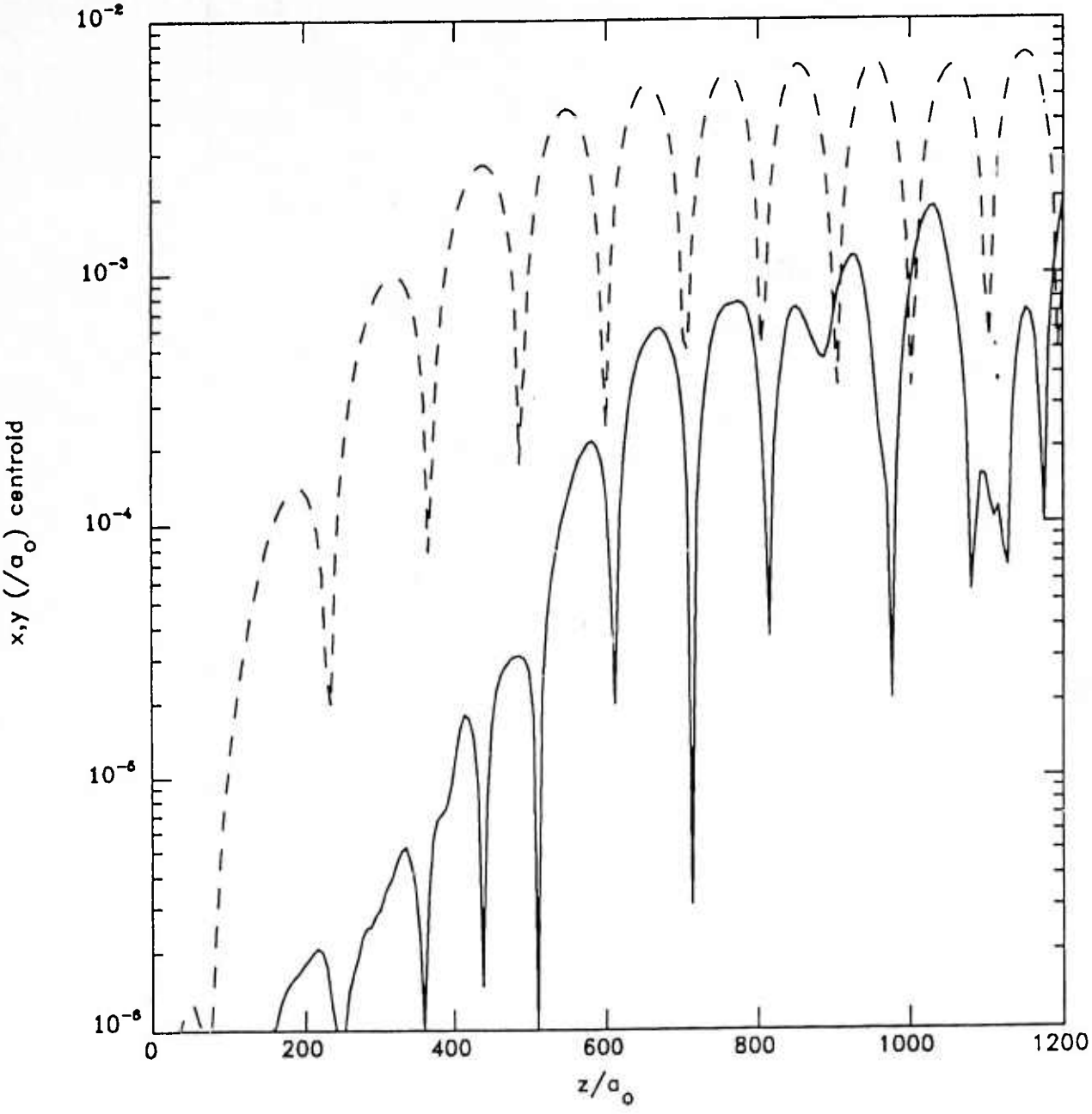

Figure 1. Plot of the beam x and y centroids at ζ = 50 cm as a function of the beam propagation distance. The initial perturbation $y_o = 10^{-5}$ so that saturation is reached while the hose instability is in the linear regime. The dashed line is the y centroid and the solid line is the x centroid. The initial perturbation is chosen in the y directions.

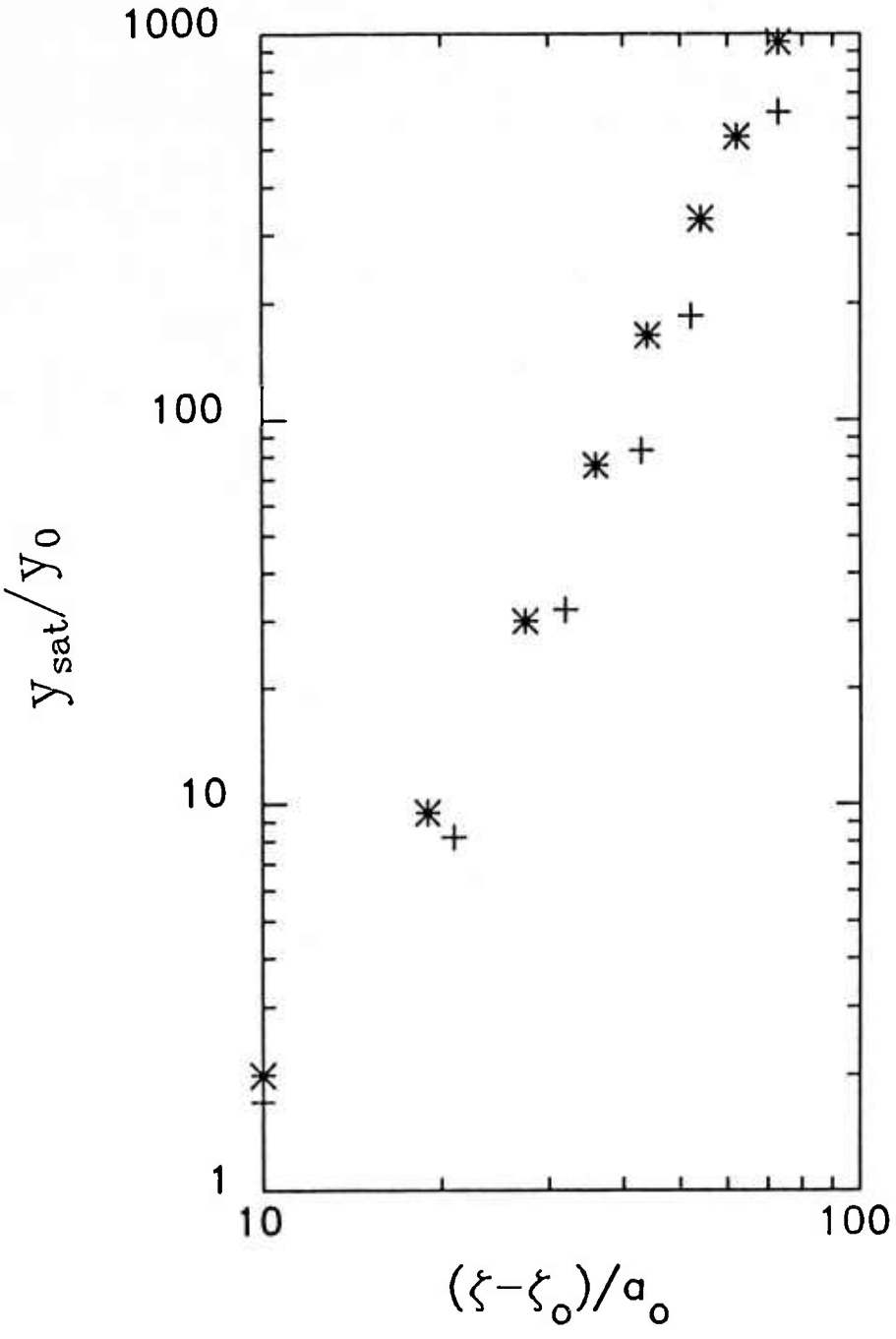

Figure 2. Plot of the saturated hose amplitude as a function of the distance back from the point of the initial perturbation. The SARLAC results are marked with *'s, while the VIPER results are marked with +'s.

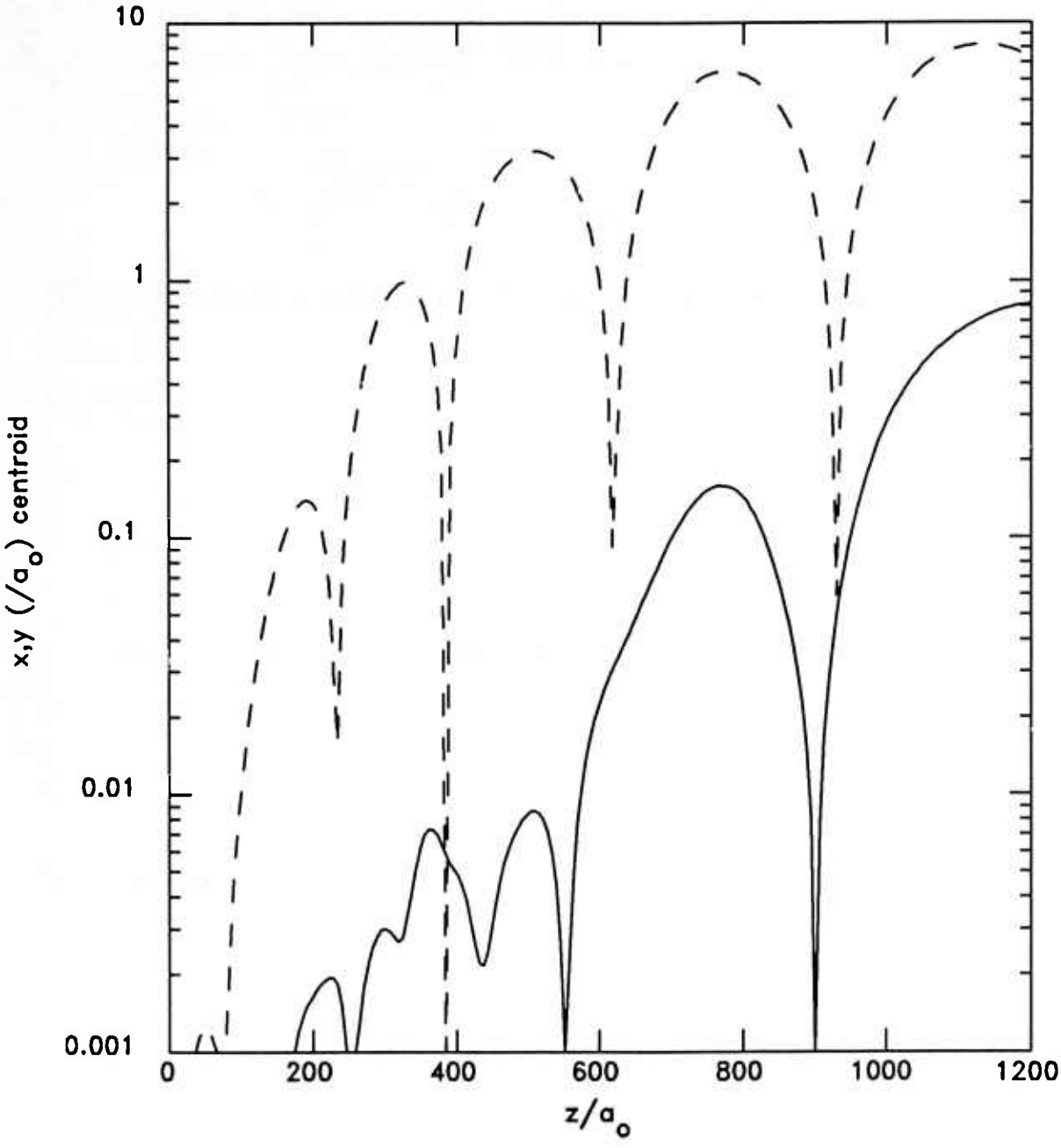

Figure 3. Plot of the beam x and y centroids at ζ = 50 cm as a function of the beam propagation distance. The initial perturbation is $y_o = 10^{-2}$ so that the hose instability becomes nonlinear. When the hose motion becomes large, the beam radius increases and the frequency of the oscillation decreases. Again, the dashed line is the y centroid and the solid line is the x centroid.

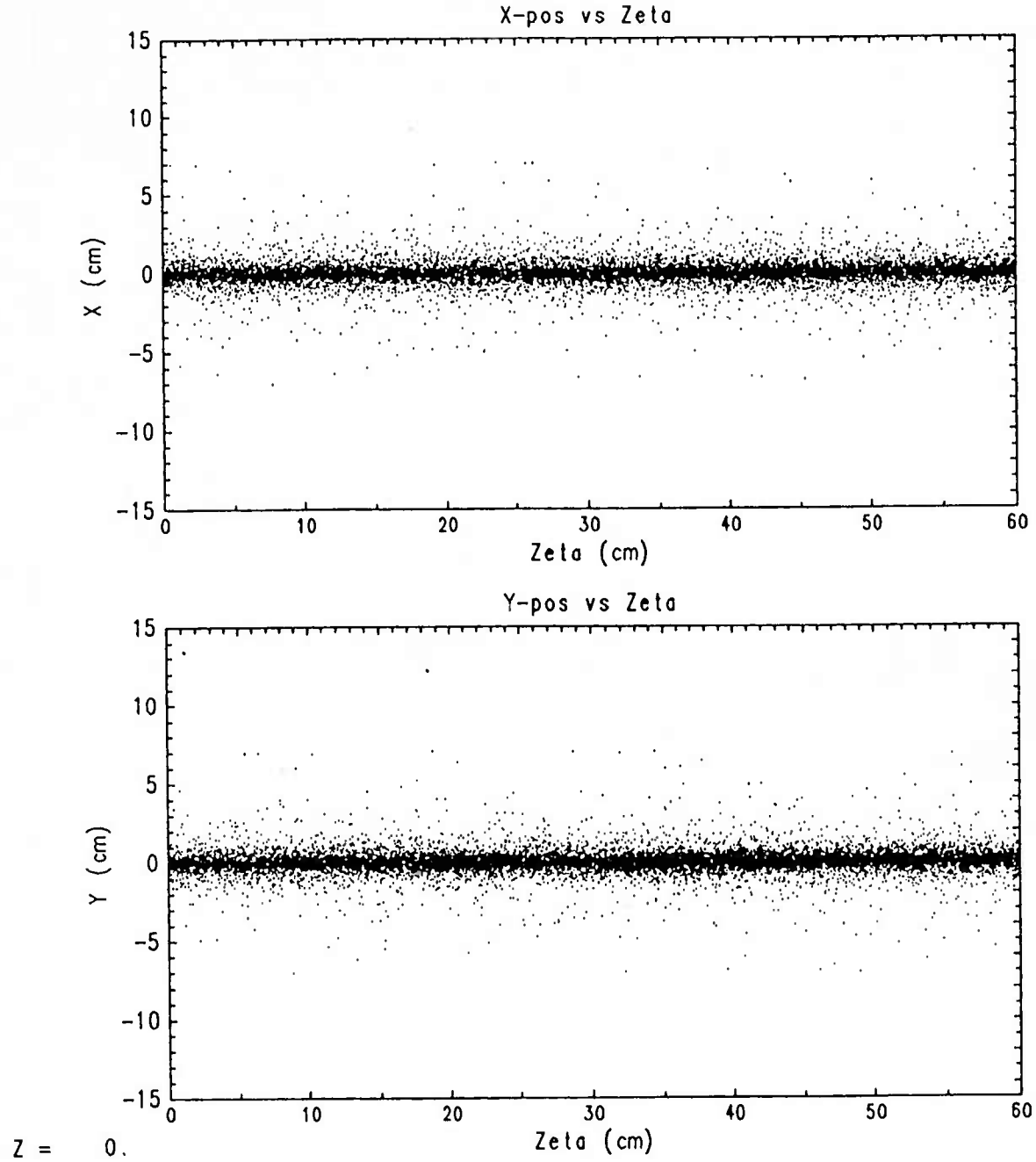

Figure 4. Plot of the beam particle positions at z = 0. The particles are loaded with a Bennett distribution. The beam current increases with increasing ζ but this is not indicated by increasing numbers of particles because the particles are weighted with the charge.

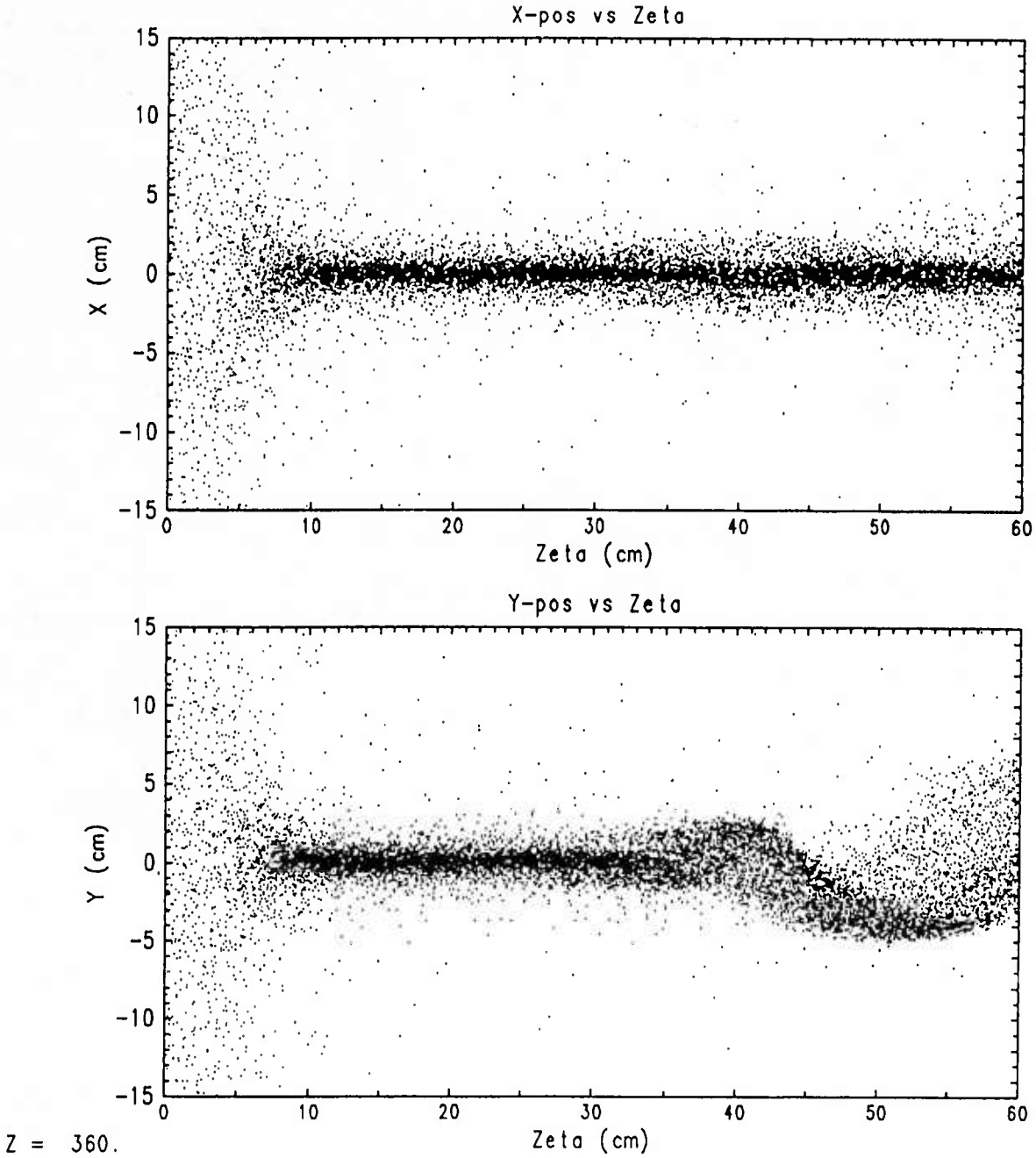

Figure 5. Plot of the beam particle positions at z = 360 cm. The beam head has begun to blow off and the hose perturbation has grown enough to be easily seen.

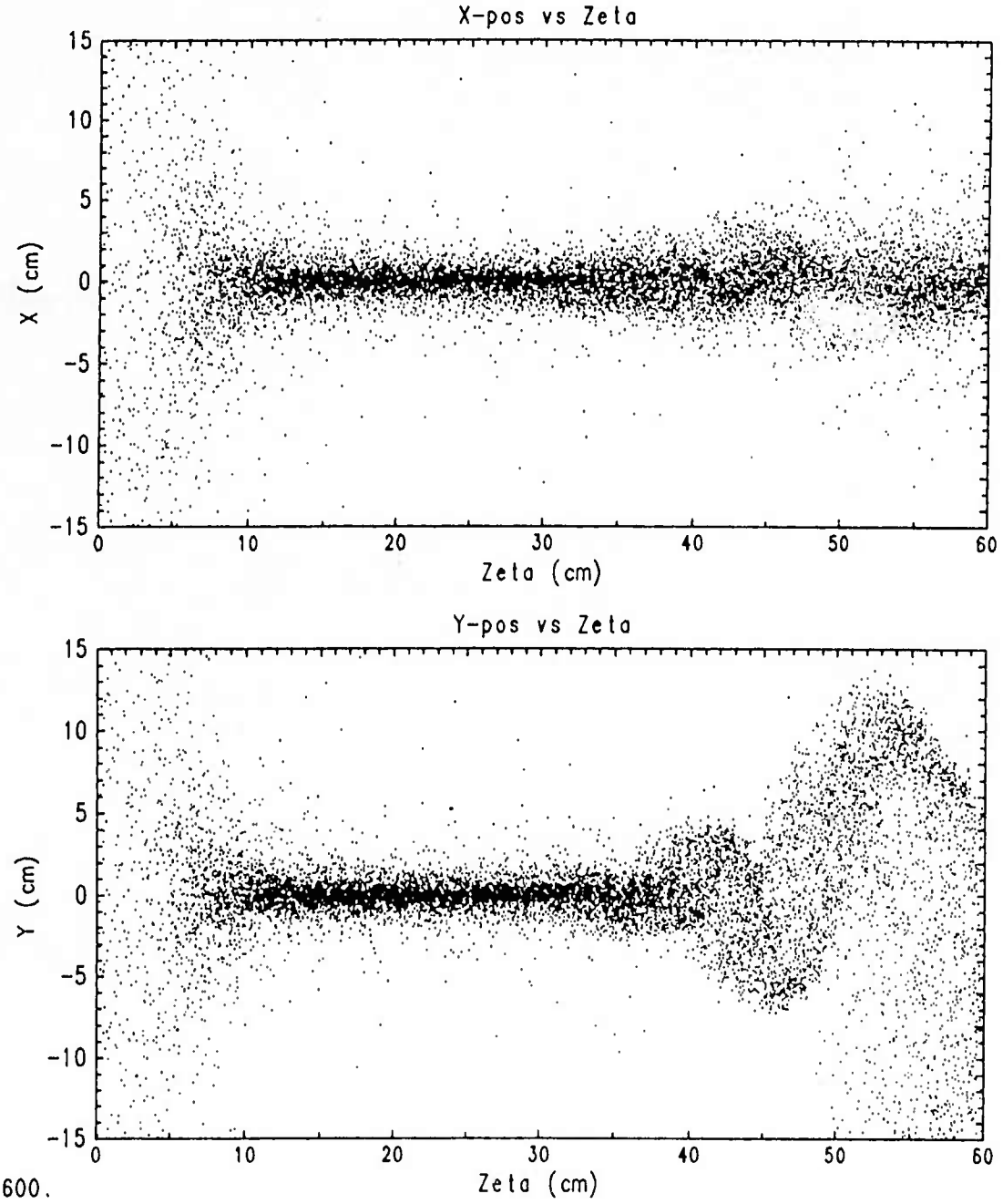

Figure 6. Plot of the beam particle positions at z = 600 cm. The hose perturbation has grown so large that the tail of the beam is completely disrupted.

Distribution List*

Naval Research Laboratory
4555 Overlook Avenue, S.W.
Attn: CAPT W. G. Clautice - Code 1000
Dr. M. Lampe - Code 4792 (20 copies)
Dr. T. Coffey - Code 1001
Head, Office of Management & Admin - Code 1005
Director of Technical Services - Code 2000
NRL Historian - Code 2604
Dr. J. Boris - Code 4040
Dr. M. Picone - Code 4040
Dr. M. Rosen - Code 4650
Dr. M. Haftel - Code 4665
Dr. S. Ossakow - Code 4700 (26 copies)
Dr. A. Ali - Code 4700.1
Dr. M. Friedman - Code 4700.1
Dr. R. Taylor - BRA (4700.1)
Mr. I. M. Vitkovitsky - Code 4701
Dr. S. Gold - Code 4740
Dr. R. Meger - Code 4750
Dr. A. Robson - Code 4760
Dr. D. Murphy - Code 4763
Dr. R. Pechacek - Code 4763
Dr. G. Cooperstein - Code 4770
Dr. D. Colombant - Code 4790
Dr. R. Fernsler - Code 4790
Dr. I. Haber - Code 4790
Dr. R. F. Hubbard - Code 4790
Dr. G. Joyce - Code 4790
Dr. Y. Lau - Code 4790
Dr. S. P. Slinker - Code 4790
Dr. P. Sprangle - Code 4790
W. Brizzi - Code 4790A
Code 4790 (20 copies)
Library - Code 2628 (2 copies)
D. Wilbanks - Code 2634
Code 1220

* Every name listed on distribution gets one copy except for those where extra copies are noted.

Air Force Office of Scientific Research
Physical and Geophysical Sciences
Bolling Air Force Base
Washington, DC 20332
Attn: Major Bruce Smith

Air Force Weapons Laboratory
Kirtland Air Force Base
Albuquerque, NM 87117
Attn: W. Baker (AFWL/NTYP)
D. Dietz (AFWL/NTYP)
Lt Col J. Head

U. S. Army Ballistics Research Laboratory
Aberdeen Proving Ground, Maryland 21005
Attn: Dr. Donald Eccleshall (DRXBR-BM)
Dr. Anand Prakash

Avco Everett Research Laboratory
2385 Revere Beach Pkwy
Everett, Massachusetts 02149
Attn: Dr. R. Patrick
Dr. Dennis Reilly

Ballistic Missile Def. Ad. Tech. Ctr.
P.O. Box 1500
Huntsville, Alabama 35807
Attn: Dr. M. Hawie (BMDSATC-1)

Chief of Naval Material
Office of Naval Technology
MAT-0712, Room 503
800 North Quincy Street
Arlington, VA 22217
Attn: Dr. Eli Zimet

Cornell University
369 Upson Hall
Ithaca, NY 14853
Attn: Prof. David Hammer

DASIAC - DETIR
Kaman Tempo
25600 Huntington Avenue, Suite 500
Alexandria, VA 22303
Attn: Mr. F. Wimenitz

Defense Advanced Research Projects Agency
1400 Wilson Blvd.
Arlington, VA 22209
Attn: Dr. Shen Shey
Dr. H. L. Buchanan

Department of Energy
Washington, DC 20545
Attn: Dr. Wilmot Hess (ER20:GTN,
High Energy and Nuclear Physics)
Mr. Gerald J. Peters (G-256)

Directed Technologies, Inc.
8500 Leesburg Pike, Suite 601
Vienna, VA 22180
Attn: Dr. Ira F. Kuhn
Dr. Nancy Chesser

C. S. Draper Laboratories
555 Technology Square
Cambridge, Massachusetts 02139
Attn: Dr. E. Olsson
Dr. L. Matson

Institute for Fusion Studies
University of Texas at Austin
RLM 11.218
Austin, TX 78712
Attn: Prof. Marshall N. Rosenbluth

Intelcom Rad Tech.
P.O. Box 81087
San Diego, California 92138
Attn: Dr. W. Selph

Joint Institute for Laboratory
Astrophysics
National Bureau of Standards and
University of Colorado
Boulder, CO 80309
Attn: Dr. Arthur V. Phelps

Kaman Sciences
1500 Garden of the Gods Road
Colorado Springs, CO 80933
Attn: Dr. John P. Jackson

La Jolla Institute
P.O. Box 1434
La Jolla, California 92038
Attn: Dr. K. Brueckner

La Jolla Institute
P. O. Box 1434
La Jolla, CA 92038
Attn: Dr. K. Brueckner

Lawrence Berkeley Laboratory
University of California
Berkeley, CA 94720
Attn: Dr. Edward P. Lee

Lawrence Livermore National Laboratory
University of California
Livermore, California 94550
Attn: Dr. Richard J. Briggs
Dr. Simon S. Yu
Dr. Frank Chambers
Dr. James W.-K. Mark, L-477
Dr. William Fawley
Dr. William Barletta
Dr. William Sharp
Dr. Daniel S. Prono
Dr. John K. Boyd
Dr. Kenneth W. Struve
Dr. John Clark
Dr. George J. Caporaso
Dr. William E. Martin
Dr. Donald Prosnitz

Lockheed Missiles and Space Co.
3251 Hanover St.
Bldg. 205, Dept 92-20
Palo Alto, CA 94304
Attn: Dr. John Siambis

Los Alamos National Scientific Laboratory
P.O. Box 1663
Los Alamos, NM 87545
Attn: Dr. L. Thode
Dr. H. Dogliani, MS-5000
Dr. R. Carlson
Ms. Leah Baker, MS-P940
Dr. Carl Ekdahl
Dr. Joseph Mack

Maxwell Laboratories Inc.
8888 Balboa Avenue
San Diego, CA 92123
Attn: Dr. Ken Whitham

McDonnell Douglas Research Laboratories
Dept. 223, Bldg. 33, Level 45
Box 516
St. Louis, MO 63166
Attn: Dr. Evan Rose
Dr. Carl Leader

Mission Research Corporation
1720 Randolph Road, S.E.
Albuquerque, NM 87106
Attn: Dr. Brendan Godfrey
Dr. Thomas Hughes
Dr. Lawrence Wright
Dr. Barry Newberger
Dr. Michael Mostrom
Dr. Dale Welch

Mission Research Corporation
P. O. Drawer 719
Santa Barbara, California 93102
Attn: Dr. C. Longmire
Dr. N. Carron

National Bureau of Standards
Gaithersburg, Maryland 20760
Attn: Dr. Mark Wilson

Naval Surface Warfare Center
White Oak Laboratory
Silver Spring, Maryland 20903-5000
Attn: Dr. R. Cawley
Dr. J. W. Forbes
Dr. B. Hui
Mr. W. M. Hinckley
Mr. N. E. Scofield
Dr. E. C. Whitman
Dr. M. H. Cha
Dr. H. S. Uhm
Dr. R. Fiorito
Dr. K. T. Nguyen
Dr. R. Stark
Dr. R. Chen

Office of Naval Research
800 North Quincy Street
Arlington, VA 22217
Attn: Dr. C. W. Roberson
Dr. F. Saalfeld

Office of Naval Research (2 copies)
Department of the Navy
Code 01231C
Arlington, VA 22217

Office of Under Secretary of Defense
Research and Engineering
Room 3E1034
The Pentagon
Washington, DC 20301
Attn: Dr. John MacCallum

ORI, Inc.
1375 Piccard Drive
Rockville, MD 20850
Attn: Dr. C. M. Huddleston

Physics International, Inc.
2700 Merced Street
San Leandro, CA. 94577
Attn: Dr. E. Goldman

Princeton University
Plasma Physics Laboratory
Princeton, NJ 08540
Attn: Dr. Francis Perkins, Jr.

Pulse Sciences, Inc.
600 McCormack Street
San Leandro, CA 94577
Attn: Dr. Sidney Putnam
Dr. John Bayless

Sandia National Laboratory
Albuquerque, NM 87115
Attn: Dr. David Hasti
Dr. Collins Clark
Dr. Barbara Epstein
Dr. John Freeman
Dr. Charles Frost
Dr. Gordon T. Leifeste
Dr. Gerald N. Hays
Dr. James Chang
Dr. Michael G. Mazerakis
Dr. John Wagner
Dr. Ron Lipinski

Science Applications Intl. Corp.
P. O. Box 2351
La Jolla, CA 92038
Attn: Dr. Rang Tsang

Science Applications Intl. Corp.
5150 El Camino Road
Los Altos, CA 94022
Attn: Dr. R. R. Johnston
Dr. Leon Feinstein
Dr. Douglas Keeley

Science Applications Intl. Corp.
1710 Goodridge Drive
McLean, VA 22102
Attn: Mr. W. Chadsey
Dr. A Drobot
Dr. K. Papadopoulos

Commander
Space & Naval Warfare Systems Command
PMW-145
Washington, DC 20363-5100
Attn: CAPT J. D. Fontana
LT Fritchie

SRI International
PS0-15
Molecular Physics Laboratory
333 Ravenswood Avenue
Menlo Park, CA 94025
Attn: Dr. Donald Eckstrom
Dr. Kenneth R. Stalder

Strategic Defense Initiative Org.
1717 H Street, N. W.
Washington, DC 20009
Attn: Lt Col R. L. Gullickson
Dr. J. Ionson
Dr. D. Duston

Strategic Defense Initiative Office
Directed Energy Weapons Office, The
Pentagon
Office of the Secretary of Defense
Washington, DC 20301-7100
Attn: Dr. C. F. Sharn (OP0987B)

Titan Systems, Inc.
9191 Towne Centre Dr.-Suite 500
San Diego, CA 92122
Attn: Dr. R. M. Dowe

University of California
Physics Department
Irvine, CA 92664
Attn: Dr. Gregory Benford

University of Maryland
Physics Department
College Park, MD 20742
Attn: Dr. Y. C. Lee
Dr. C. Grebogi

University of Michigan
Dept. of Nuclear Engineering
Ann Arbor, MI 48109
Attn: Prof. Terry Kammash
Prof. R. Gilgenbach

Director of Research
U.S. Naval Academy
Annapolis, MD 21402 (2 copies)